

RESEARCH MEMORANDUM

COMPARISON OF CALCULATED AND MEASURED THERMAL
DISTORTIONS IN A REACTOR CONTROL ROD FOR
TEMPERATURE PATTERNS SIMULATING TWO
REACTOR OPERATING CONDITIONS

By Tibor F. Nagey

Lewis Flight Propulsion Laboratory
Cleveland, Ohio

LIBRARY COPY

MAY 23 1958

LANGLEY AERONAUTICAL LABORATORY
LIBRARY, NACA
LANGLEY FIELD, VIRGINIA

NATIONAL ADVISORY COMMITTEE
FOR AERONAUTICS
WASHINGTON

April 1953

Declassified April 1958

NACA RM E53B26

NATIONAL ADVISORY COMMITTEE FOR AERONAUTICS

RESEARCH MEMORANDUM

COMPARISON OF CALCULATED AND MEASURED THERMAL DISTORTIONS IN A
REACTOR CONTROL ROD FOR TEMPERATURE PATTERNS SIMULATING
TWO REACTOR OPERATING CONDITIONS

By Tibor F. Nagey

SUMMARY

The results of a simplified theoretical analysis are presented of the calculated distortion of a stainless-steel-clad silver-cadmium control rod under the influence of several temperature patterns, and these results are also compared with the measured distortions for the same temperature patterns.

The calculated distortion for a temperature variation simulating reactor operation with 50-percent shim rod insertion agreed with the measured values for about the first 60 percent of the rod (measured from the fixed end) and underpredicted the free end motion by about 0.016 inch.

The calculated distortion for the maximum temperature gradient case (roughly simulating reactor operation with shim rods out) proved to be a relatively good faired curve for the measured data (within 0.002 in.).

INTRODUCTION

An investigation was conducted at the NACA Lewis laboratory to determine the thermal distortion as caused by temperature distribution associated with unsymmetrical heat production in a control rod for the Argonne Naval Reactor. The experimental results of these tests are reported in references 1 to 3. The present report presents calculated distortions corresponding to measured temperature patterns, and the calculated and experimental results are compared for several temperature patterns.

2879

CF-1

SYMBOLS

- L length of segment, in.
- T_0 environmental temperature, $^{\circ}\text{R}$
- T_1 cold side segment temperature, $^{\circ}\text{R}$
- T_2 hot side segment temperature, $^{\circ}\text{R}$
- w width of segment (or zone), in.
- ΔL increase in length of segment, in.
- δ distortion of segment, in.
- ϵ coefficient of linear expansion, in./in.- $^{\circ}\text{F}$

Subscripts:

- n number of segments
- T total number of segments for four zones
- t total number of segments for one zone

METHOD AND PROCEDURE

Description of control rod. - Figure 1(a) shows a diagrammatic sketch of the cross section of the control rod and gives the construction details. The control rod consisted of a 25-75 percent cadmium-silver core, clad with stainless steel. The rod cross-section was in the shape of a cross having a span of 4 inches. The total arm thickness was $7/32$ inch consisting of $1/8$ -inch core alloy with a stainless steel cladding thickness of $3/64$ inch. After fabrication, the rod was hot-rolled in order to form a bond between the core alloy and the stainless steel. The rod was stress-relieved.

Figure 1(b) shows several views of the control rod with the locations of the thermocouples. The over-all length of the rod was $53\frac{3}{4}$ inches.

The control rod was mounted vertically with the fixed end at the bottom; strain gages were located near the clamped end to ensure freedom from initial stress while clamping.

Method of obtaining nonsymmetrical temperature patterns. - The control rod was heated by a 75 KVA induction heater. Axial temperature distributions were obtained by varying the axial spacing of the heater coil turns. Transverse temperature gradients were obtained by making the heating coil and the rod nonconcentric and by a series of air jets mounted along the rod and directed toward the center of the cross. A schematic sketch and a photograph showing the heating system in detail is given in references 1 to 3.

Method of measuring distortion. - Distortion of the rod was measured by means of dial indicators. Normally two indicators were located at each tip of the cross in positions along the length of the rod. The indicators were mounted on four vertical supports fastened to the same mounting plate as the control rod. These supports were protected from conduction and radiation to eliminate thermal distortion in the supports themselves. Dial indicators were also supplied to indicate any motion of these supports. Fused quartz rods, 12 inches long, were used to transmit the motion of the control rod to the dial indicators. The use of fused quartz eliminated the need for a correction for thermal expansion of the indicator rods. The reproducibility of the indicator readings was within ± 0.002 inch.

Temperature distribution. - Temperature patterns were measured by means of 104 thermocouples distributed between 8 stations located along the axis of the rod as shown in figure 1(b). At several stations thermocouples were mounted oppositely on each face of the $7/32$ -inch-thick plate (e.g., thermocouples 4 and 6, fig. 1(b)); while at the intersection of the two plates forming the cross, four thermocouples were located in the corners (e.g., thermocouples 3, 7, 11, 15, fig. 1(b)). For these cases the arithmetic average value of the temperatures was used.

In order to simplify the presentation of the temperature patterns the control rod is assumed to be two independent $7/32 \times 4 \times 53\frac{3}{4}$ -inch flat plates.

Figures 2(a) and 2(b) show a typical variation of temperature plotted against plate width for eight longitudinal positions (case I of table I run 1). The figure shows two plots, one for each plate of the cross.

A cross plot of figure 2 was used to get the longitudinal variation of temperature at each longitudinal zone boundary. In this way a complete temperature profile of the rod was obtained.

The thermocouple location, the associated temperatures, and the measured distortions of references 2 and 3 are listed in table I for two typical cases. Case I of table I lists two values from reference 2,

2879

CF-1 back

where the temperature pattern was intended to simulate reactor operation with 50-percent shim rod insertion. Case II of table I lists two runs from reference 3 where the temperature pattern roughly simulated reactor operation with the shim rods out.

Method of calculating distortion. - The following assumptions were used in this analysis:

- (1) The control rod was assumed to be homogeneously composed of type 347 stainless steel.
- (2) The control rod was assumed to behave as two independent $7/32 \times 4 \times 53\frac{3}{4}$ -inch flat plates. (Hence, there were no mutual restraining effects in distortion.)
- (3) The control rod temperature across the $7/32$ -inch dimension was assumed to be constant.
- (4) Sufficiently small transverse segments of the plate were chosen for analysis in order that an assumption of a linear temperature gradient across each segment in the transverse direction could be made and, further, that each segment would be small enough in a longitudinal direction that the temperature gradient in that direction could be taken as zero.

Figure 3(a) is a schematic drawing showing the four 1-inch zones into which each plate was divided. This particular division of the plate was determined by the location of thermocouples; that is, the temperature of the boundary of each zone is known.

Analysis of the temperature data of references 2 and 3 showed that a segment length of 1 inch had to be used in order to approximate conditions where no longitudinal temperature variation existed.

Figure 3(b) is a schematic drawing showing the manner in which each plate of the rod was subdivided in order to meet the requirements of assumption 4. Hence, each zone of the four zones comprising a single plate consists of 53 segments each $1 \times 1 \times 7/32$ inch and one segment $1 \times 3/4 \times 7/32$ inch.

The distortion for each zone was calculated independently of the adjacent zones by the following method.

If a bar of length L has its temperature uniformly raised, and is allowed to expand free from any constraint, the increase in length ΔL is

$$\Delta L = L\epsilon(T_1 - T_0) \quad (1)$$

A constant value of the coefficient of linear expansion ϵ of 9.48×10^{-6} inch per inch per $^{\circ}\text{F}$ for type 347 stainless steel was used in all the calculations. This constant value was within 0.5 percent of the correct value for the range of temperatures encountered.

A list of symbols and their units are given in the section entitled Symbols.

Figure 4 shows a segment ($1 \times 1 \times 7/32$ in.) of one zone of the plate, with sides (a) and (b) of the segment being at different temperatures. The differential change in length of the two sides is given by:

$$\Delta(\Delta L) = L\epsilon(T_2 - T_1) \quad (2)$$

This differential increase in length can be assumed to cause the segment to tilt and the angle of tilt (fig. 4) is given by:

$$\theta = \tan^{-1} \frac{\Delta(\Delta L)}{w} \quad (3)$$

where w is always taken as 1 inch.

The distortion of this segment is then defined as the distance δ , that the reference corner (α) (fig. 4) moved from its original position on the vertical axis. Thus,

$$\delta = L[1 + \epsilon(T_2 - T_1)] \sin \theta \quad (4)$$

The equation for the distortion of any segment, n , may be written:

$$\delta_n = L[1 + \epsilon(T_2 - T_1)_n] \sin \sum_{1}^n \theta \quad (5)$$

The total distortion of a zone of the plate away from its original vertical position is:

$$\delta_t = \sum_{1}^n \delta \quad (6)$$

In order to calculate the distortion of one plate of the cross-shaped rod, this procedure is repeated for each of the four zones, and an average value of δ_T is calculated as follows:

$$(\delta_T)_n = \left(\frac{\delta_{t,1} + \delta_{t,2} + \delta_{t,3} + \delta_{t,4}}{4} \right)_n \quad (7)$$

This same procedure is then repeated for the remaining plate of the cross. The distortion of the plate, the ends of which are labeled 1 and 9 in figure 1(b), is always plotted as a change in the y direction, while distortion of the plate labeled 5 and 13 is always plotted as a change in the x direction.

RESULTS AND DISCUSSION

Comparison of calculated and measured distortions. - The measured distortion as reported in reference 2 and the calculated distortions are shown in figure 5 as functions of longitudinal position on the control rod. Figure 5(a) shows the comparison for the motion in the y direction, and figure 5(b) shows the comparison for the x direction. In both cases, only one longitudinal edge of the plate (stations 1 and 5, as given in figs. 5(a) and 5(b), respectively) is plotted. The temperature distribution curves on which these thermal distortion calculations are based are shown in figure 2. The sample calculations included in appendix A show the stepwise manner by which the calculated curve of figure 5(a) was obtained.

In figure 5(a) the calculated distortion in the y direction matches the trend of the measured data for about 60 percent of the length of the rod very closely. Near the free end of the rod, however, the measured value of distortion is about 0.016 inch greater. The calculated distortion in the x direction (fig. 5(b)) agreed within 0.010 inch with the measured data for the entire length of the rod.

Figure 6 shows the same type of comparison as in the previous figure, with the measured values of distortion taken from reference 3 (table I, case II). However, the maximum temperature gradient across the plate for the case shown in figure 6 was greater than the temperature gradient in figure 5(a), causing the motion in the y direction to be about four times greater. The distortion in the x direction remained about the same for both cases.

In figure 6 the calculated curve is seen to represent the measured distortion with good accuracy. The calculated curve matches the measured data over the entire length within 0.002 inch. The distortions as measured and calculated in the x direction match within 0.010 inch.

SUMMARY OF RESULTS

The results of a theoretical analysis of the thermal distortion of a stainless-steel-clad silver-cadmium control rod under the influence of several temperature patterns compared with the measured distortions for the same temperature patterns are as follows:

1. The calculated distortion for a temperature variation simulating reactor operation with 50-percent shim rod insertion agreed with the measured values for about the first 60 percent of the rod (measured from the fixed end) and underpredicted the free end motion by about 0.016 inch.

2. The calculated distortion for the maximum temperature gradient case (roughly simulating reactor operation with shim rods out) proved to be a relatively good faired curve for the measured data (within 0.002 in.).

Lewis Flight Propulsion Laboratory
National Advisory Committee for Aeronautics
Cleveland, Ohio, February 4, 1953

The total distortion for all four zones is as follows:

$$(\delta_T)_1 = \frac{\delta_{t,1} + \delta_{t,2} + \delta_{t,3} + \delta_{t,4}}{4} = \frac{0.0002 - 0.0001 - 0.0001 - 0.0002}{4} = 0$$

where

$$z = 53.75$$

$$(\delta_T)_2 = \frac{\delta_{t,1} + \delta_{t,2} + \delta_{t,3} + \delta_{t,4}}{4} = \frac{0.0007 - 0.0002 - 0.0006 - 0.0005}{4} = \bar{0}.0001$$

where

$$z = 53.0$$

$$(\delta_T)_3 = \frac{0.0015 - 0.0004 - 0.0012 - 0.0009}{4} = \bar{0}.0002$$

where

$$z = 52.0$$

$$(\delta_T)_4 = \frac{0.0026 - 0.0007 - 0.0019 - 0.0015}{4} = \bar{0}.0004$$

where

$$z = 51.0$$

$$(\delta_T)_{54} = \frac{0.0168 - 0.0540 - 0.0452 - 0.0122}{4} = \bar{0}.024$$

where

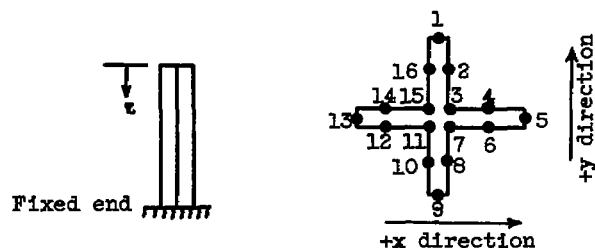
$$z = 1.0$$

REFERENCES

1. Nagey, T. F., and Lietzke, A. F.: Measurement of Distortion in First Experimental Control Rod for Argonne Naval Reactor. NACA RM E51A30, 1951.
2. Lietzke, A. F., and Nagey, T. F.: Measurement of Distortion in Second Experimental Control Rod with Temperature Patterns Simulating Shim Rod Out and Shim Rod 50 Percent Inserted for Argonne Naval Reactor. NACA RM E51E25, 1951.
3. Nagey, T. F., and Lietzke, A. F.: Measurement of Distortion in Second Experimental Control Rod for Argonne Naval Reactor with Constant Transverse Temperature Gradient and Uniform Longitudinal Temperature Distribution. NACA RM E51H10, 1951.

TABLE I. - DISTORTION AND TEMPERATURE DATA

(a) Case I (data from ref. 2)

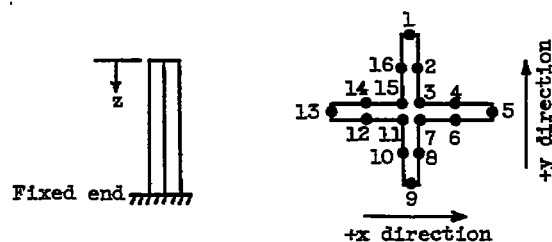


z, in.	Run number	Temperature, °F															
		Thermocouple location															
		1	2	3	4	5	6	7	8	9	10	11	12	13	14	15	16
1	1	459	461	461	461	458	458	459	454	451	449	450	449	437	417	456	460
	2	460	463	464	464	459	459	459	457	451	451	451	450	438	426	457	460
8	1	480				475	476	456	466	467				464	471	459	480
	2	481				475	475	455	465	467				462	470	468	481
15	1	493	493	460	479	485	485	446	474	483	478	487	482	483	482	462	488
	2	495	495	465	480	486	487	449	477	486	482		484	485	486	466	489
22	1	500				487	487	448	470	473				480	480	469	435
	2	503				490	490	451	473	475				482	483	473	445
29	1	483	485	477	477	473	473	465	474	474	474	469	479	479	480	477	484
	2	485	485	479	479	476	475	467	475	475	475	470	480	480	481	480	485
36	1	464				462	464	464	459	469				466	466	466	464
	2	465				463	463	465	469	469				466	465	466	466
43	1	443	444	445	445	448	445	445	445	444	444	446	443	440	440	445	445
	2	446	446	447	448	447	447	448	448	446	446	449	446	444	443	446	446
50	1	441				441	449	456	446	436				436	447	462	465
	2	449				453	459	469	456	445				445	458	472	478

z, in.	Run number	Distortions	
		Motion in y direction	Motion in x direction
		Station 1	Station 5
2	1	-0.039	0.0000
	2	-0.040	0.002
10	1	-0.029	0.005
	2	-0.030	0.006
20	1	-0.008	0.005
	2	-0.009	0.006
35	1	-0.003	0.009
	2	-0.004	0.010
52	1	0.002	0.007
	2	0.001	0.006

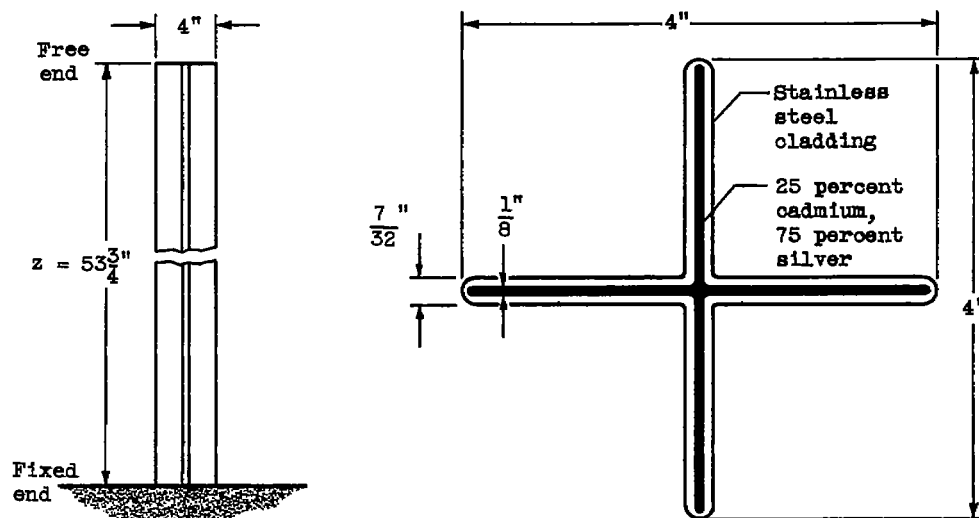
TABLE I. - Concluded. DISTORTION AND TEMPERATURE DATA

(b) Case II (data from ref. 3)

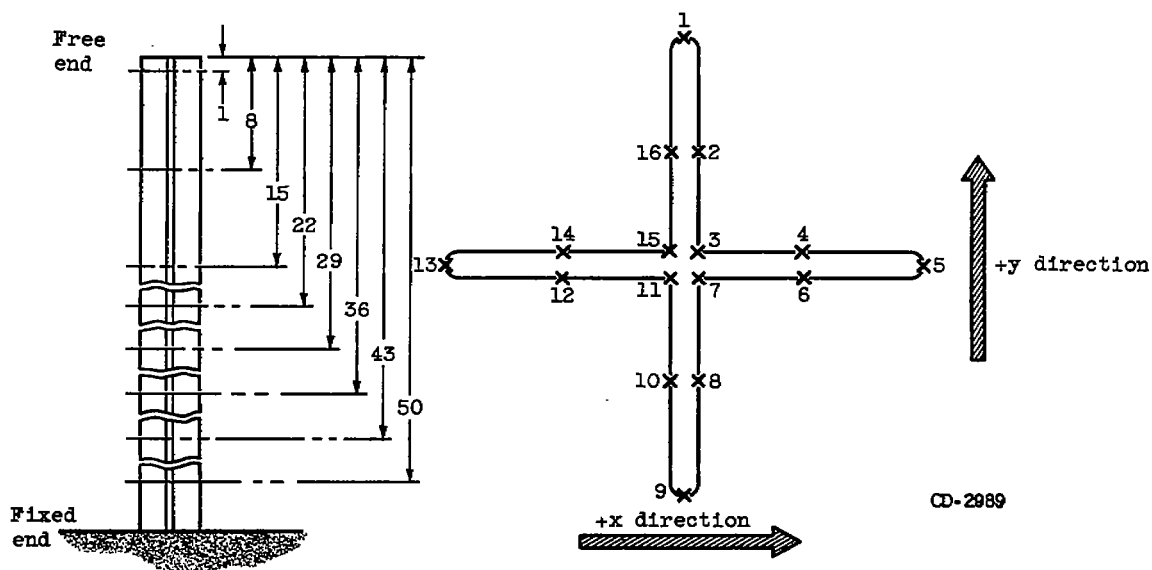


z, in.	Run number	Temperature, °F															
		Thermocouple location															
		1	2	3	4	5	6	7	8	9	10	11	12	13	14	15	16
1	1	449	448	426	429	414	418	419	398	387	400	395	415	409	358	426	449
	2	444	446	433	431	422	425	412	404	366	386	387	414	401	369	407	444
8	1	450				430	436	421	393	388				421	421	421	445
	2	445				435	435	424	388	385				408	407	405	425
15	1	451	452	443	448	445	430	423	430	416			440	446	445	440	455
	2	454	456	454	453	453	437	432	429				451	450	450	450	455
22	1	454				435	430	413	412	416				439	369	430	424
	2	454				432	433	420	409	395				406	377	406	406
29	1	463	457	430	450	453	452	432	430	418	429	420	436	434	437	435	454
	2	469	463	453	456	459	459	452	444	435	435	410	413	414	415	441	457
36	1	465				439	430	420	419	415				451	450	441	455
	2	466				444	434	417	407	406				412	419	426	457
43	1	464	461	447	452	462	454	428	431	442	430	437	460	463	460	451	463
	2	474	474	470	470	470	470	439	444	449	449	449	464	470	470	469	469
50	1	457				405	415	415	426	406				410	422	433	454
	2	469				407	407	405	408	406				405	414	444	461

z, in.	Run number	Distortions	
		Motion in y direction	Motion in x direction
		Station 1	Station 5
2	1	-0.168	0.004
	2	-0.171	-0.009
10	1	-0.120	0.004
	2	-0.123	0.000
20	1	-0.066	0.007
	2	-0.074	-0.001
35	1	-0.031	0.006
	2	-0.031	0.002
52	1	0.001	0.003
	2	-0.002	0.002

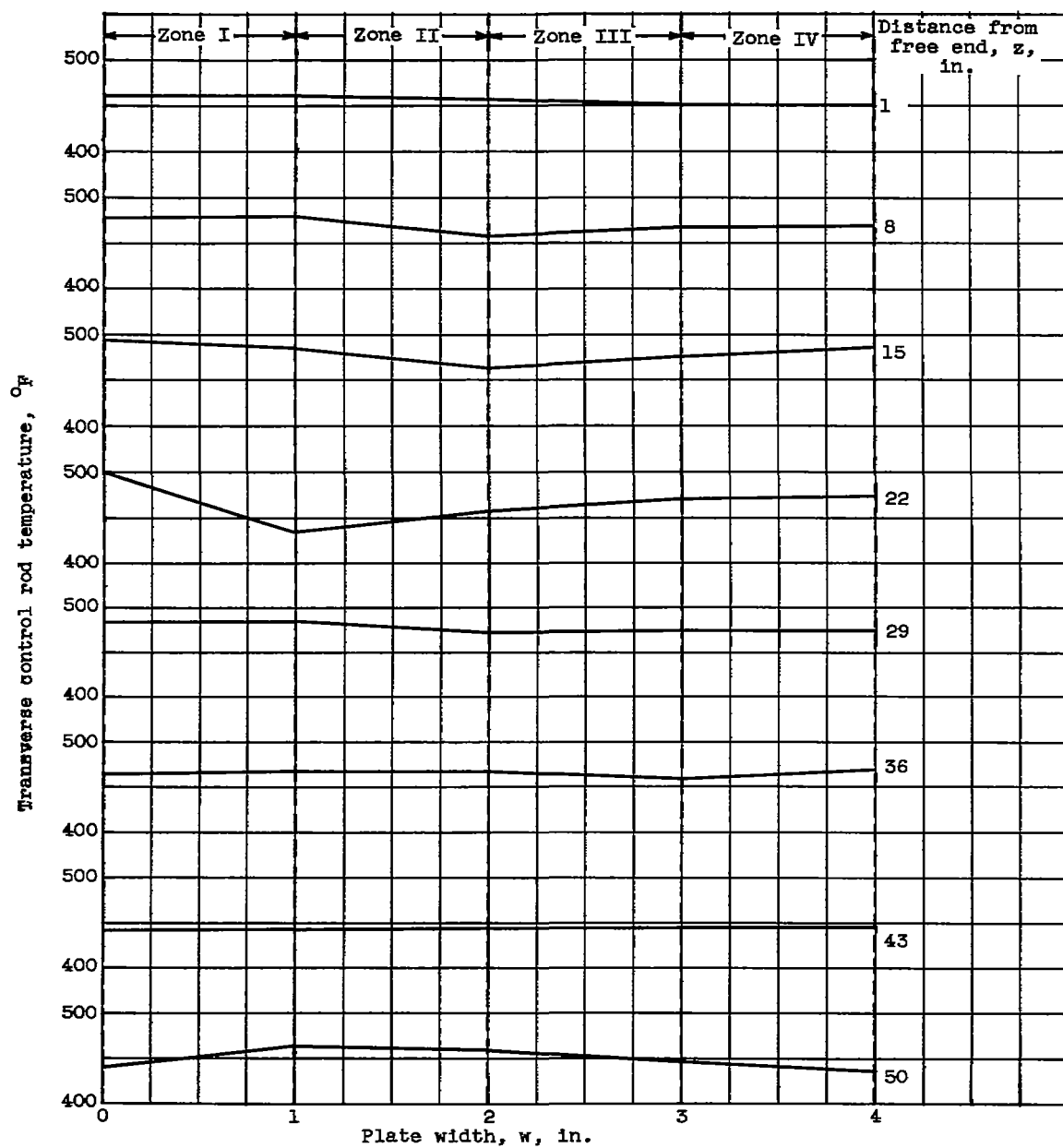


(a) Diagrammatic sketch of control rod.



(b) Sketch showing longitudinal and transverse thermocouple locations.

Figure 1. - Diagrammatic sketch showing construction and instrumentation details of control rod.



(a) Transverse temperature pattern from station 1 to station 9 (table I, case I, run 1).

Figure 2. - Variation of control rod temperature with plate width at several longitudinal positions.

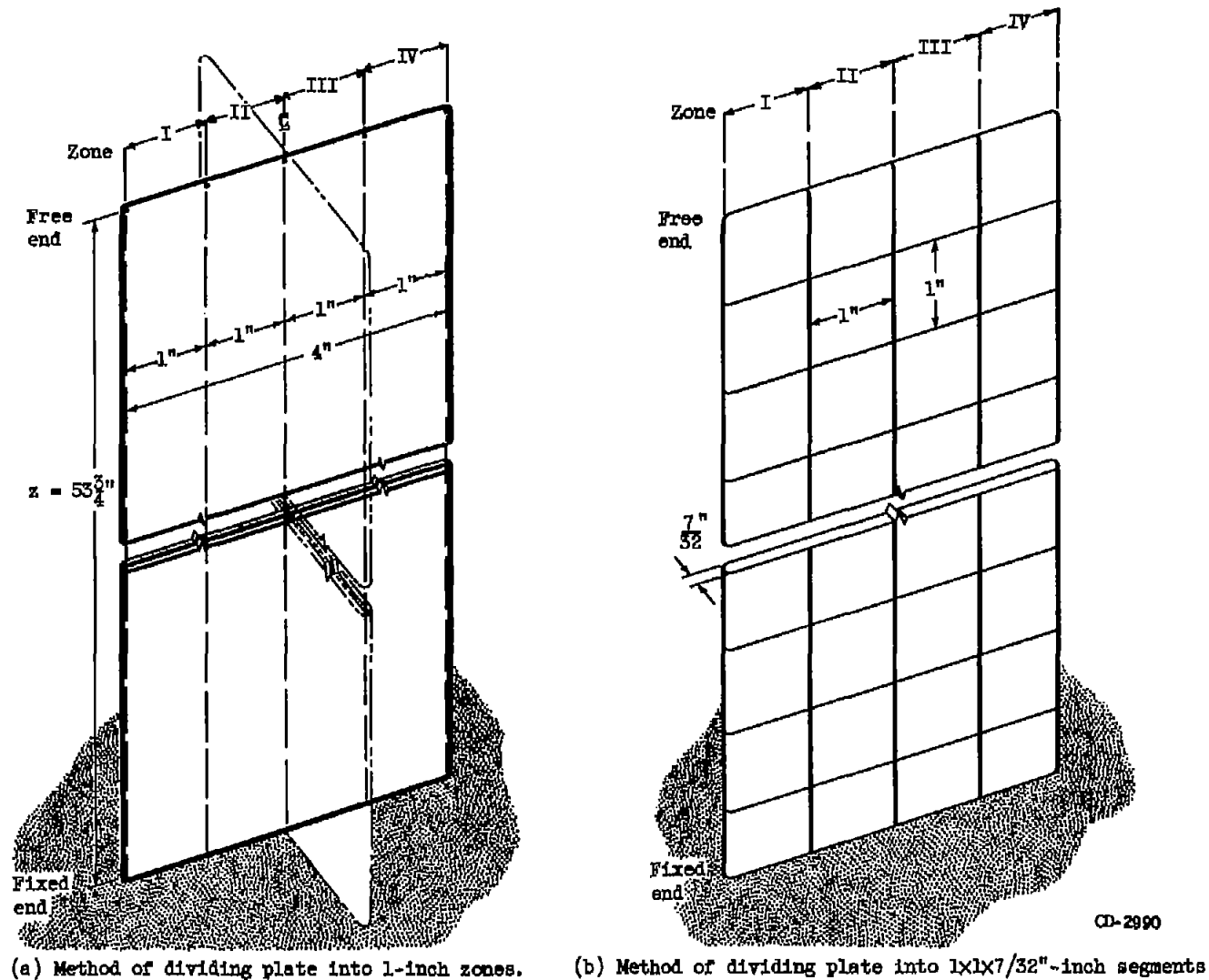


Figure 3. - Sketch showing manner in which control rod was subdivided for analysis.

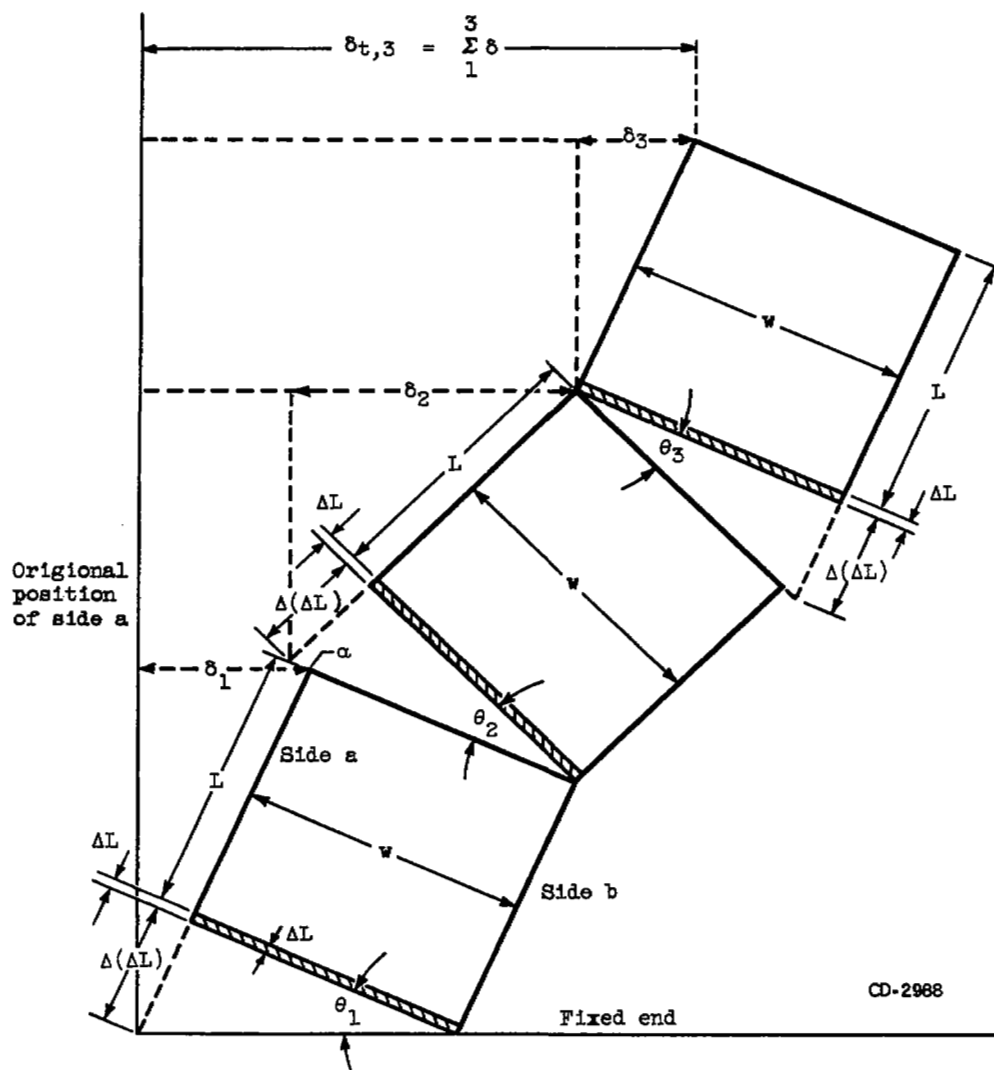


Figure 4. - Sketch showing trigonometric method of treating distortion of the segments of one zone.

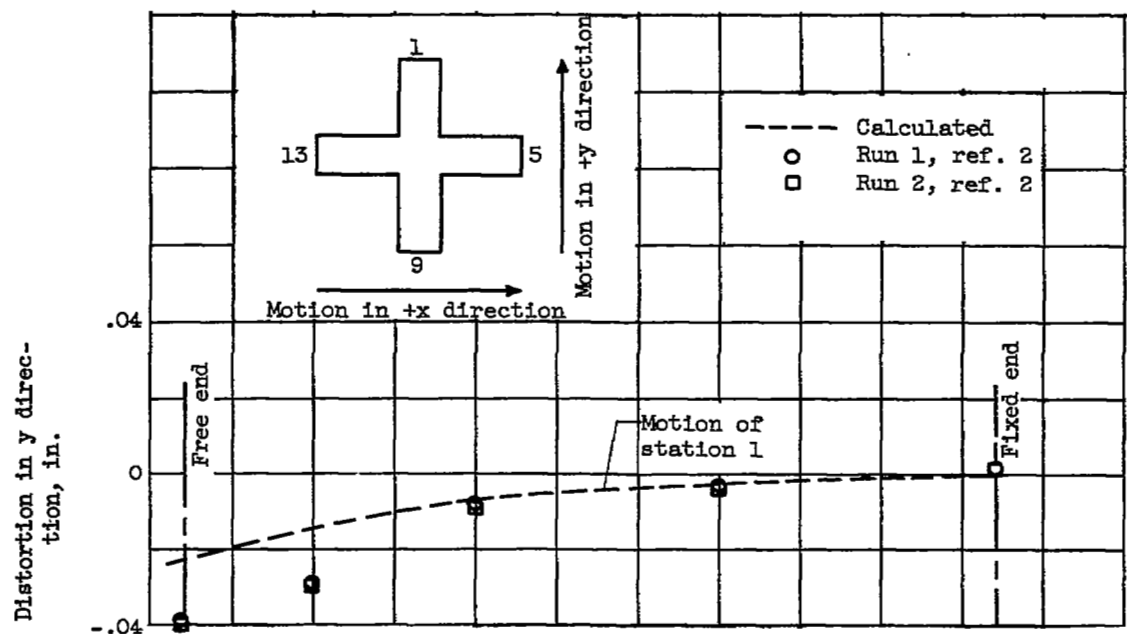
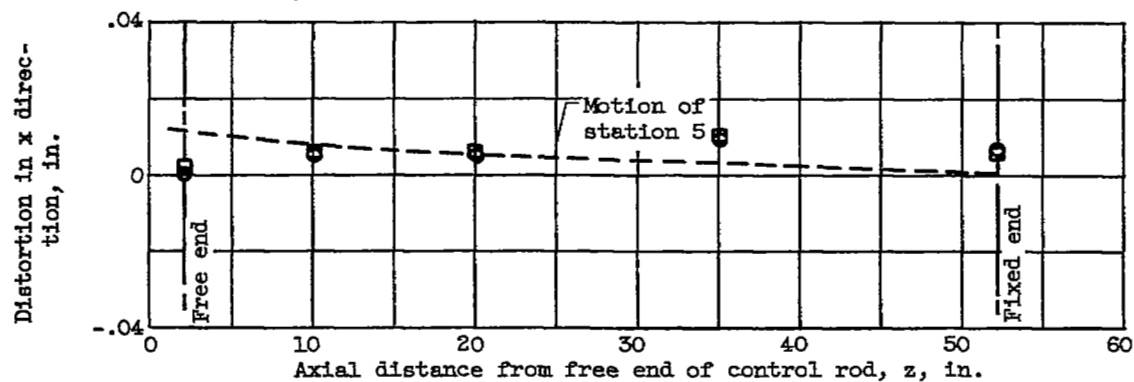
(a) Variation of distortion in y direction with z .(b) Variation of distortion in x direction with z .

Figure 5. - Calculated distortion of control rod compared with measured distortions of reference 2.

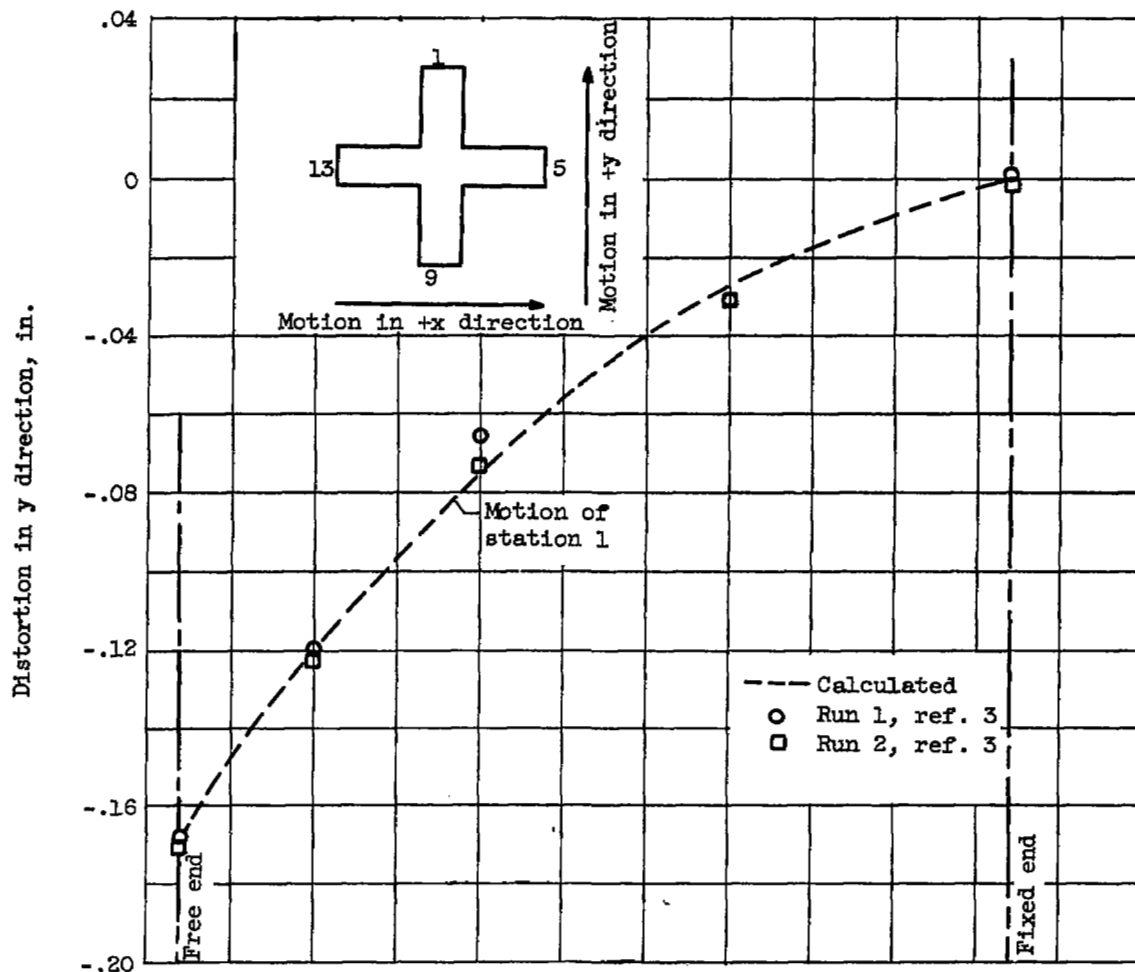
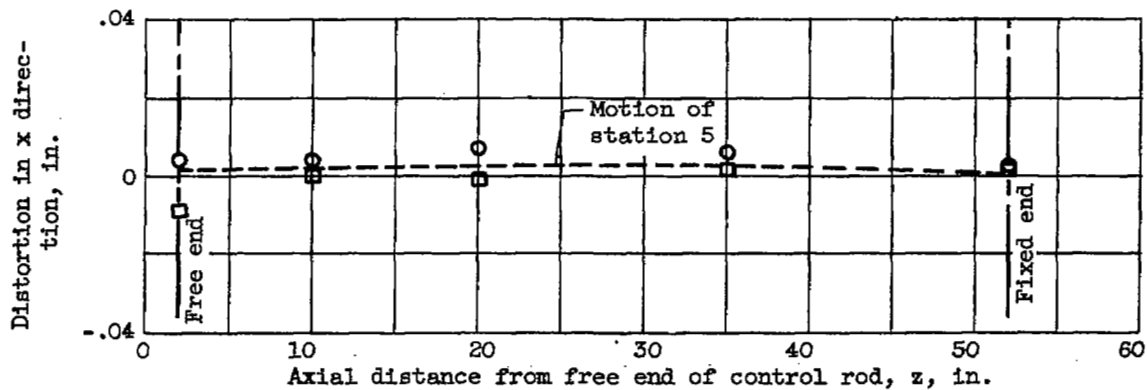
(a) Variation of distortion in y direction with z .(b) Variation of distortion in x direction with z .

Figure 6. - Calculated distortion of control rod compared with measured distortions of reference 3.

NASA Technical Library



3 1176 01435 6852